

Experimental Electrical Characterization of High Speed Interconnects

Steven B. Goldberg, Michael B. Steer, Paul D. Franzon, and Jettory S. Kasten

High Frequency Electronics Laboratory
Department of Electrical and Computer Engineering
North Carolina State University
Raleigh, NC 27695-7911.

ABSTRACT

As clock speeds increase, electrical simulation of interconnects becomes essential in engineering design. In spite of the availability of a variety of electromagnetic modeling tools, experimental characterization is required to verify and, in some cases, to develop models of lines and interconnect discontinuities for use in simulation. In this paper we present measurement techniques to experimentally characterize the electrical performance of interconnects on printed circuit boards and multi-chip modules. Novel techniques are presented for calibrated measurements of two-port and three-port structures. Measurements of a transmission line, a via, and a tee on a printed circuit board are presented.

INTRODUCTION

Present day high-end printed circuit board (PCB) and multichip module (MCM) based digital systems require that transmission line and discontinuity effects be incorporated in transient system simulation. High speed digital signals have significant frequency components up to RF and microwave frequencies. A signal with a rise time of t_r has significant frequency components up to a frequency $f_{max} = 0.35N/t_r$, where $N = 5$ for most digital systems. Accurate interconnect simulation, therefore, requires accurate interconnect models up to f_{max} [2]. Thus signals with a rise time of 1 ns, for example, require models up to at least 1.75 GHz. With the improved packaging obtained with MCMs and advanced VLSI devices, models valid at yet higher frequencies will be required.

The traditional approach to interconnect model development is to fit physically-based analytic models to detailed field theoretic simulations. In the case of transmission lines, this is only possible provided that two dimensional stability is maintained and that the cross-section is highly regular. Then quasi-static analysis yields capacitance and inductance per unit length parameters. For discontinuities quasi-static analysis yields lumped element equivalent circuit models. Using a perturbation assumption, corrections are made for frequency dependent effects such as the skin effect. Extending field theoretic models to handle full three dimensional structures and including frequency dependent effects is not at all straightforward and a major penalty is incurred in terms of simulation time. In any case experimental verification is required to obtain confidence in the validity of models of interconnect structures.

The measurement requirements for PCBs and MCMs are somewhat relaxed compared to measurements of microwave circuits, however, typically many measurements are required to calibrate models, to investigate the characteristics of various nonhomogenous PCB and MCM technologies, and to investigate statistical variations. Furthermore MCM and PCB interconnects are lossy so that traditional planar circuit calibration techniques which require lossless line standards can not be directly used. The purpose of this paper is to present an experimental procedure suited to characterization of interconnect discontinuities on PCBs and MCMs. In particular techniques are developed for calibrated two-port and three-port measurements using novel calibration schemes.

TWO-PORT CALIBRATION

At RF and microwave frequencies, significant measurement errors are introduced by fixturing. In the case of two-port measurements these errors can be removed by inserting known standards. This can be conveniently done in a coaxial line-based measurement system as precisely known standards, (e.g terminations, lowloss delay lines, etc.) are readily available. However,

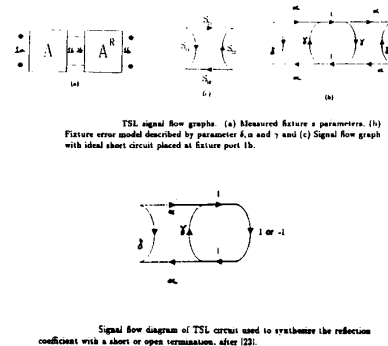
precisely known standards are not available for calibration of a planar measurement system such as an MCM or PCB. The calibration of both vector automatic network analyzers and test fixturing is required to accurately determine the scattering parameters of a device under test (DUT).

The TRL technique is the preferred method for characterizing the fixtures of a planar measurement system [3, 5]. The primary reason for this is that a matched load, or precisely known termination, is not required in the calibration procedure. Instead a through connection, an arbitrary reflection and a reference transmission line are used as standards and these are easily modeled and constructed. The arbitrary reflection need not be precisely known as long as it is large and can be repeatably placed at the internal ports of the test fixtures. In this paper it is shown that that this standard can be synthesized when the two fixtures are identical yielding a symmetrical through connection — hence the term through-symmetry-line (TSL) calibration. Close matching of the test fixtures can readily be achieved up to low microwave frequencies and at higher frequencies through careful design. This is combined with our previously published enhanced-through-reflect-line (ETRL) calibration scheme [4].

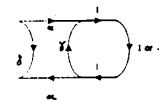
TSL

A typical microstrip fixture is a first order symmetric fixture if identical coax to microstrip transitions and identical microstrip line lengths exist. These can be achieved into low microwave frequencies and at higher frequencies through careful design. A first order symmetric fixture is one that is reciprocal and the port 1 and port 2 reflection coefficients are equal, however the error network for each port is not symmetric. See fig.1a. Therefore, the fixture can be represented with three error terms, and so three standards are needed.

Symmetry permits synthesis of TRL reflection standards thereby eliminating their need. The reflection is arbitrary and is typically a short circuit. For the symmetrical through connection, we can



TSL signal flow graphs. (a) Measured fixture s parameters. (b) Fixture error model described by parameter δ , α and γ and (c) Signal flow graph with ideal short circuit placed at fixture port 1b.



Signal flow diagram of TSL circuit used to synthesize the reflection coefficient with a short or open termination, after [2].

Figure 1:

TSL signal flow graphs. (a) Symmetric fixture signal flow graph, and (b) Signal flow graph with ideal short circuit placed at fixture port 1.

calculate the reflection coefficient with the microstrip ports terminated in ideal open or short circuits.

In the signal flow graphs of fig. 1b, we consider the through connection s parameters given by, $S_{11f}(= S_{22f})$ and $S_{21f}(= S_{12f})$, and the actual parameters of the A network being δ , α and γ for S_{11a} , $S_{21a} = S_{12a}$ and S_{22a} respectively. In addition, the input reflection coefficient with an ideal short circuit placed at port 1 of A is

$$\rho_{sc} = \delta - \frac{\alpha^2}{1 + \gamma} \quad (1)$$

Using Mason's rule to relate the fixture parameters to the individual network parameters, we have the results

$$S_{11f} = \delta + \frac{\alpha^2 \gamma}{1 - \gamma^2} \quad (2)$$

$$S_{21f} = \frac{\alpha^2}{1 - \gamma^2} \quad (3)$$

Combining (1), (2) and (3), the short circuit reflection coefficient can be expressed as a function of fixture s parameters (measured).

$$\rho_{sc} = S_{11f} - S_{21f} \quad (4)$$

A similar result holds for an ideal open circuit placed at port 1b.

$$\rho_{oc} = S_{11f} + S_{21f} \quad (5)$$

ρ_{sc} and ρ_{oc} can be derived for any fixture that exhibits at least first order symmetry including other planar measurement fixtures. Since these reflection coefficients are derived mathematically, it is possible to "insert" ideal open and short circuits within a non-insertable medium such as a dielectric loaded waveguide with the use of only two standards.

Enhanced Through-Symmetry-Line - ETSL

The development of ETRL was necessary because of assumptions inherent to the TRL algorithm. The algorithm requires the characteristic impedance of the line standard to be equal to the measurement system impedance. If not, then its value has to be determined. Also, the algorithm assumes a pure real characteristic impedance with no frequency dependence. However, most fixtures are dispersive and it becomes necessary to determine the complex characteristic impedance Z_c as a function of frequency. ETSL determines the complex characteristic impedance using the space capacitance of the microstrip geometry and an experimentally determined propagation constant, $\gamma = \alpha + j\beta$, in the same way as ETRL, but uses synthesized reflection coefficients instead of measured ones. Details in the development of ETRL can be seen in [4].

TWO-PORT RESULTS

Synthesized Short

A 3000 mil microstrip transmission line was tested to determine the error networks of the coaxial to microstrip transitions using ETSL. The network analyzer was calibrated to the coaxial reference planes C1 and C2 (as shown in fig. 4) using the network analyzer Open Short Load calibration procedure for application of a two-tier measurement system. A transmission line and a standard through was connected to the coaxial reference planes and a short circuit reflection coefficient was synthesized. To verify the synthetic reflection standard, a low inductance short circuit was placed at the microstrip reference plane M1, shown on fig. 4. The measured short circuit reflection coefficient is compared in magnitude with the synthesized value in fig. 2. The magnitude minimum is slightly different between measured and calculated. This minimum corresponds to the resonance of the discontinuity capacitance with the inductive input impedance of the short circuit terminated microstrip. Moreover, the physical short has a parasitic inductance that will lower the resonant frequency from the ideal synthesized short. In fact, it may be possible to extract an inductance value from this frequency shift. In any event, the TRL reflection standard can be synthesized

Transmission line

After the second reference plane was established, a 5000 mil transmission line was characterized and the complex characteristic impedance was calculated. Fig. 3 shows the real part of this impedance. Note that the impedance drops at low frequencies and levels to a stable value. This is due to the lack of resolution of the line length at those frequencies. The stable value of the

real part of the characteristic impedance is about 59 Ω . A better value closer to the designed value of 50 Ω can be achieved with inclusion of the DC resistance to the transmission line impedance model. This will be presented in a yet to be published paper.

Via

With the transmission line now characterized with the ETSL algorithm, a pi equivalent circuit was determined for a PCB via. See fig. 4.

The pi equivalent circuit was extracted from the de-embedded via s parameters. This extraction was done by converting the via

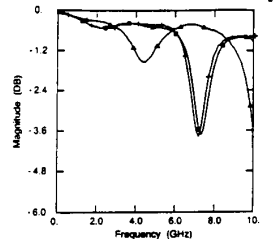


Figure 2: Magnitude comparison of synthesized and measured short circuit at microstrip reference plane. (+) Measured short circuit reflection coefficient, (\Delta) synthesized and (\square) synthesized open circuit reflection coefficient.

Figure 2: Magnitude comparison of synthesized and measured short circuit at microstrip reference plane. (+) Measured short circuit reflection coefficient, (\Delta) synthesized and (\square) synthesized open circuit reflection coefficient.

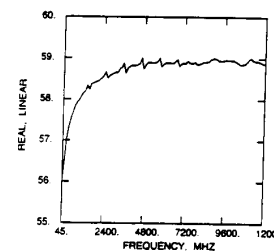


Figure 3: Characteristic impedance real part of a 5000 mil transmission line using synthetic standards.

Figure 3: Characteristic impedance real part of a 5000 mil transmission line.

s parameters to admittance parameters, which form a pi equivalent circuit, and then inverting these admittances. The resulting shunt capacitance (in pico Farads) and series inductive reactance (in ohms) are shown in fig. 5.

When interpreting the TSL results, we should consider the fact that we have imposed a pi equivalent model to the via and at higher frequencies this result will decrease in accuracy. The series reactance behaves as an inductor through two GHz and the capacitance is constant to five GHz. The increasing capacitance (with frequency) is associated with the increased energy stored in the fringe electric fields and the non-ideal inductance arises from resonances with other parasitic capacitances.

THREE-PORT CALIBRATION

Three-port calibration and characterization of a device must be performed using two-port measurements with the additional port terminated. Traditionally three-port DUTs are deembedded from the test fixture using Wood's renormalization technique [7]. This method however becomes inaccurate when the termination on the additional port strays when fixturing presents significant discontinuities so that the termination does not present a real impedance to the DUT's third port. In our approach, two sets of terminations are used to obtain near optimum deembedding whereby transmission measurements are used to determine trans-

mission parameters and reflection measurements are used to determine reflection parameters.

Fig. 6 is a simplistic representation of a three port device. Since only two-port measurements are available, each of the ports must be terminated in a standard with known reflection coefficient for every combination of measurements. Fig. 6 also shows a full signal flowgraph for a three port. A partially terminated three port yields a relationship between the s parameters of the three port, S_{ij} , the measured two-port s parameters, S_{ij}^M , and the reflections of the terminations Γ_k . Using Mason's non-touching loop theorem, the equation for the two-port reflection s parameter at the i^{th} node is:

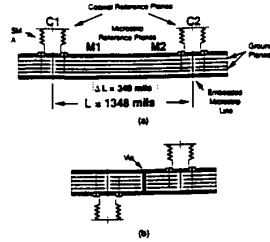


Figure 4:

Diagram of the fixture with line standard inserted (a) and via (b).

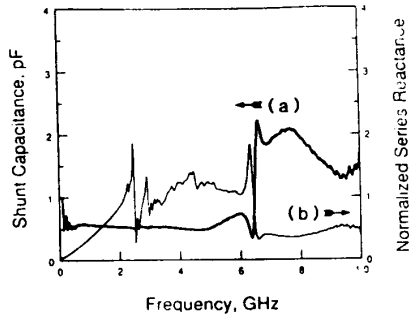


Figure 5:

a) Via shunt capacitance and b) series reactance normalized to 50Ω .

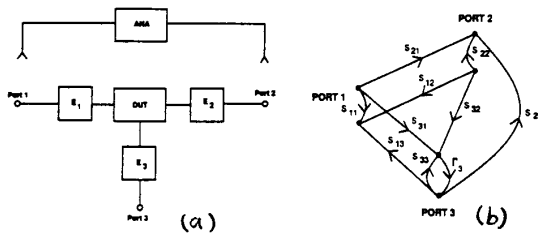


Figure 6:

a) Simple model of a three port device. b) Signal flow graph of a three port device with port 3 terminated by reflection coefficient, Γ .

$${}^{mk}S_{ij}^M = S_{ij} + \frac{S_{ki} {}^m\Gamma_k S_{ik}}{1 - S_{kk} {}^m\Gamma_k} \quad (6)$$

Similarly

$${}^{mk}S_{ij}^M = S_{ij} + \frac{S_{kj} {}^m\Gamma_k S_{ik}}{1 - S_{kk} {}^m\Gamma_k} \quad (7)$$

In both equations, M indicates that the s parameter is a measured quantity, and m and k are indices distinguishing different terminations ${}^m\Gamma_k$ at port k. The equations describe 3 sets of two-port S parameter measurements with $i, j, k = 1, 2, 3; i \neq j \neq k$. This leads to 12 coupled nonlinear equations which have multiple solutions. The equations can also be poorly conditioned as the measured two-port s parameters may only be determined to 1% accuracy. This is especially so if the magnitude of one three-port s parameter is much less than that of another since then the small s parameters may be lost in the equation solution process. That is, it may not be possible to determine s parameters that are small relative to other s parameters.

In general, good accuracy is obtained when S_{ii} (S_{ij}) is evaluated solely in terms of ${}^{mk}S_{ii}^M$ (S_{ij}^M) measurements as, usually, they are of the same order. This requires that two different reflection standards be used at each port (so that $m = 1, 2$) and

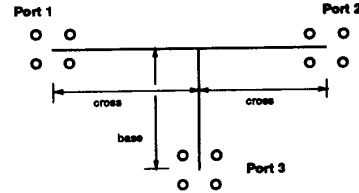


Figure 7:

Configuration of a microstrip tee with arms on the same plane of a PCB.

that two-port S parameter measurements be taken for all two-port combinations (that is $i, j, k = 1, 2, 3; i \neq j \neq k$). This leads to 24 equations which can be solved as a linear set of equations so that

$$S_{ii} = \frac{{}^1\Gamma_k {}^2\Gamma_k ({}^{2k}S_{ii}^M - {}^{1k}S_{ii}^M) ({}^1\Gamma_i {}^{2i}S_{kk}^M - {}^{2i}S_{kk}^M) - ({}^1\Gamma_i - {}^{2i}\Gamma_i) ({}^1\Gamma_k {}^{2k}S_{ii}^M - {}^{2k}S_{ii}^M)}{{}^1\Gamma_k {}^2\Gamma_k ({}^{2k}S_{ii}^M - {}^{1k}S_{ii}^M) {}^1\Gamma_i {}^{2i}S_{kk}^M - ({}^1\Gamma_i - {}^{2i}\Gamma_i) ({}^1\Gamma_k {}^{2k}S_{ii}^M - {}^{2k}S_{ii}^M)} \quad (8)$$

and

$$S_{ij} = \frac{({}^1\Gamma_k {}^{2k}S_{ij}^M - {}^{2i}S_{ij}^M) - S_{kk} {}^1\Gamma_k {}^2\Gamma_k ({}^{2k}S_{ij}^M - {}^{1k}S_{ij}^M)}{{}^1\Gamma_k - {}^{2i}\Gamma_k} \quad (9)$$

where S_{kk} is found from (8). A more expanded development is given in [9].

THREE-PORT RESULTS

A microstrip tee in the configuration in fig. 7 was measured two ports at a time with the unused port terminated in either 50Ω or a short. Fig. 8 is a sample of this data. This data and all its brethren was deembedded with the ETSL technique as described in the previous section.

With the deembedded data and the partially decascaded termination data that the embedded circuit sees on the extraneous port (see [9] for details), we now have all the data required to fully characterize the microstrip tee. A total of 14 measurements are required, recognizing the reciprocity circuit in this case.

Fig. 9 is a portion of the results that characterize the microstrip tee in the configuration in fig. 7. It is interesting to note that the reflection parameters are around a value of approximately 0.33 which coincides with a 50Ω transmission line looking into parallel 50Ω loads. Also note that S_{11} and S_{22} track together closely, therefore S_{22} was omitted from the plot, while S_{33} loosely follows. This mimicry decreases with frequency, probably due to the increasing coupling of the base arm with the two cross arms. The reciprocity that is expected due to the physical

configuration of the circuit is evident, although no assumption of such was made in the algorithm. The spikes that appear are

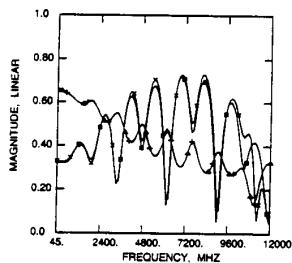


Fig. 8. Embedded s parameters of a microstrip tee with port 3 terminated with a 50 Ω load. Magnitude of (□) S_{11} , (Δ) S_{12} , (+) S_{21} , and (\times) S_{22} .

Figure 8: Embedded s parameters of a microstrip tee with port 3 terminated in nominal 50 Ω load. Magnitude of (□) S_{11} , (Δ) S_{12} , (+) S_{21} , and (\times) S_{22} .

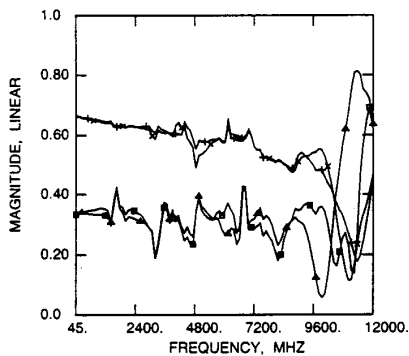


Figure 9:

Characterized microstrip tee s parameters. Magnitude of (□) S_{11} , (Δ) S_{33} , (+) S_{31} , and (\times) S_{32} .

probably due to resonances from the transmission line lengths of the arms in the tee as well as interactions of the inductive and capacitive coupling in the arms. These inductive and capacitive differences are more evident at the high frequencies.

CONCLUSION

Symmetrical calibration methods were developed to combat the non-insertable nature of printed circuit board measurement, i.e. use a minimum number of standards and do so without physically inserting them. Through-Symmetry-Line was possible because the PCB fixture was symmetric allowing a third standard to be synthesized from two standards namely the through and line. The synthesized short circuit was experimentally verified indicating that symmetry can be used to reduce the number of standards.

TSL was enhanced by calculating the complex characteristic impedance of the line standards in the same way as in ETRL and the transmission line parameters for an embedded microstrip were subsequently determined. These results were used to deembed the pi equivalent circuit of a PCB via.

An algorithm that accurately characterizes any three-port device was introduced. It is closed form and makes no assumptions

(i.e. reciprocal transmission characteristics) upon the device under test, except for linearity. It takes into consideration the influences of reflections from untested ports and returns a full characterization of the device as it is seen in the circuit. Symmetry arguments were used to do the two-port deembedding and a microstrip tee was fully characterized.

ACKNOWLEDGEMENT

This work was supported in part by a National Science Foundation Grant No. ECS-8657836 and by BNR.

REFERENCES

- [1] G.L. Matthaei, K. Kiziloglu, N. Dagli, and S.I. Long, "The nature of the charges, currents, and fields in and about conductors having cross-sectional dimensions of the order of a skin depth," *IEEE Trans. Microwave Theory Tech.*, MTT-38, August 1990, pp. 1031-1036.
- [2] L.L. Moresco, "Electronic system packaging: the search for manufacturing the optimum in a sea of constraints," *IEEE Trans. Components, Hybrids, and Manufacturing Technology*, September 1990, pp. 494-508.
- [3] G.F. Engen and C.A. Hoer, "Thru-Reflect-Line: An Improved Technique for Calibrating the Dual Six-Port Automatic Network Analyzer," *IEEE Trans. Microwave Theory Tech.*, MTT-27, December 1979, pp. 987-993.
- [4] J.S. Kasten, M.B. Steer, and R. Pomerleau, "Enhanced through-reflect-line characterization of two-port measuring systems using free-space capacitance calculation," *IEEE Trans. Microwave Theory and Tech.*, Vol. 38, No. 2, Feb. 1990, pp. 215-217.
- [5] C.A. Hoer and G.F. Engen, "Calibrating a Dual Six-Port or Four-Port for Measuring Two-Ports with any Connectors," *IEEE MTT-S International Microwave Symposium Digest*, 1986, pp. 665-668.
- [6] R.A. Speciale, "A Generalization of the TSD Network Analyzer Calibration Procedure, Covering n-Port Scattering Parameter Measurements, Affected by Leakage Errors," *IEEE Trans. Microwave Theory Tech.*, Vol. MTT-25, December 1977, pp. 1100-1115.
- [7] D. Woods, "Multiport-Network Analysis by Matrix Renormalization Employing Voltage-Wave S-Parameters with Complex Normalisation," *IEE Proc.*, Vol. 124, March 1977, pp. 198-204.
- [8] P.C. Sharma and K.C. Gupta, "A Generalized Method for De-Embedding of Multiport Networks," *IEEE Trans. Inst. Meas.*, Vol. IM-30, December 1981, pp. 305-307.
- [9] S.B. Goldberg, M.B. Steer, and P.D. Franzon, "Accurate experimental characterization of three-ports," *1991 IEEE MTT-S International Microwave Symposium Digest*, June 1991.
- [10] D. Winkelstein, M.B. Steer and R. Pomerleau, "Simulation of the Transient Response of Arbitrary Transmission Line Networks with Nonlinear Terminations," *IEEE Trans. on Circuits and Systems*, April 1991.